journal of the mechanical behavior of biomedical materials 146 (2023) 106072

Contents lists available at ScienceDirect

Journal of the Mechanical Behavior of Biomedical Materials

journal homepage: www.elsevier.com/locate/jmbbm

Thermal modulation of skin friction at the finger pad

Alessandro Valenza [a,b], Konrad Rykaczewski [c,d], Daniel M. Martinez [c], Antonino Bianco [b], Silvia Caggiari [e], Peter Worsley [e], Davide Filingeri [a,*]

[a] ThermosenseLab, Skin Sensing Research Group, School of Health Science, University of Southampton, UK
[b] Sport and Exercise Sciences Research Unit, SPPEFF Department, University of Palermo, Italy
[c] School for Engineering of Matter, Transport and Energy, Arizona State University, 501 E Tyler Mall, Tempe, AZ, 85287, USA
[d] Julie Ann Wrigley Global Futures Laboratory, Arizona State University, Tempe, AZ, 85287, USA
[e] PressureLab, Skin Sensing Research Group, School of Health Science, University of Southampton, UK

ARTICLE INFO

Keywords:
Skin temperature
Friction
Pressure ulcer
Optical coherence tomography
Computational modelling
Biophysics

ABSTRACT

Preliminary human studies show that reduced skin temperature minimises the risk of mechanically induced skin damage. However, the mechanisms by which cooling enhances skin tolerance to pressure and shear remain poorly understood. We hypothesized that skin cooling below thermo-neutral conditions will decrease kinetic friction at the skin-material interface. To test our hypothesis, we measured the friction coefficient of a thermally pre-conditioned index finger pad sliding at a normal load (5N) across a plate maintained at three different temperatures (38, 24, and 16 °C) in 8 healthy young adults (29±5y). To quantify the temperature distribution of the skin tissue, we used 3D surface scanning and Optical Coherence Tomography to develop an anatomically representative thermal model of the finger. Our group-level data indicated that the sliding finger with thermally affected tissues (up to 8 mm depth) experienced significantly lower frictional forces ($p<0.01$) at plate temperatures of 16 °C (i.e. 32% decrease) and 24 °C (i.e. 13% decrease) than at 38 °C, respectively. This phenomenon occurred consistently across participants (i.e. N = 6/8, 75%) and without large changes in skin hydration during sliding. Our complementary experimental and theoretical results provide new insights into thermal modulation of skin friction that can be employed for developing thermal technologies to maintain skin integrity under mechanical loading and shearing.

1. Introduction

Pressure ulcers (PUs) constitute a localized damage to the skin resulting from prolonged periods of pressure and shear forces, and represent a significant public health challenge, due to their impact on individuals' quality of life and the associated financial burden on healthcare providers (Coleman et al., 2014). Indeed, in the United Kingdom alone, the annual cost of treating chronic skin wounds, including PUs, has been estimated to be approximately £8.3 billion (Guest et al., 2020).

Exposure to prolonged mechanical loading on the skin can arise from several situations, including periods in lying and sitting postures and the prolonged attachment of medical devices. The associated pressure and shear forces acting on the skin induce internal tissue deformations, causing changes to the physiology of skin and sub-dermal tissue. The negative impacts of the deformation include ischemia in the blood vasculature, lymphatic impairment, and direct deformation damage (Worsley et al., 2020). In addition, the moisture level, and the temperature within and around skin tissues strongly influence skin tolerance to mechanical loading. For example, elevated humidity at the skin interface reduces the mechanical stiffness and strength of the skin and can increase its friction coefficient (André et al., 2010; Gerhardt et al., 2008). In contrast, lower-than-normal temperature reduces skin tissue's metabolic demands and could increase skin's physiological tolerance to pressure-induced damage (Clark et al., 2018). Indeed, early animal (Kokate et al., 1995) and preliminary human (Jan 2020; Tzen et al., 2013) studies show that reduced skin temperature minimises the risk of PU formation (Worsley and Bader, 2019a). While this evidence highlights the potential therapeutic role of skin cooling for maintaining tissue health, the mechanisms by which cooling enhances skin tolerance to pressure, shear, and friction remain poorly understood (Lachenbruch, 2005). An improved understanding of the fundamental mechanisms

* Corresponding author. ThermosenseLab, Skin Sensing Research Group (SSRG), Clinical Academic Facility | Level A, Room AA83 | South Academic Block (MP11), Southampton General Hospital | Tremona Road | SO16 6YD, School of Health Science, University of Southampton, UK.
E-mail address: d.filingeri@soton.ac.uk (D. Filingeri).

https://doi.org/10.1016/j.jmbbm.2023.106072
Received 23 February 2023; Received in revised form 25 April 2023; Accepted 11 August 2023
Available online 12 August 2023

underlying the physiological tolerance of human skin to mechanical loading could lead to the development of cost-effective, personalised solutions to promote skin health.

Since heating the skin increases its friction at a low normal load (0.5N)(Choi et al., 2022), we hypothesized that skin cooling below thermo-neutral conditions will decrease friction at the skin-material interface. We know that higher static friction can lead to an increased shear stress, which in turn increases the risk of PU formation under mechanical loading (Coleman et al., 2014). Yet, the role of kinetic friction in the formation of PU and friction wounds, as well as its modulation by temperature, remain little investigated, despite the pressure, the type of relative motion, the sliding velocity, as well as the local microclimate are all factors known to affect friction during dynamic skin-material interactions (Gerhardt et al., 2008). Accordingly, the aim of this study was to investigate the temperature-dependence of kinetic friction across a broad range of non-noxious skin-interface temperatures (i.e. 38 to 16 °C). To test our hypothesis, we measured the coefficient of friction (CoF) of a thermally pre-conditioned human index finger sliding at a normal load (5N) across a plate maintained at three different temperatures. While other body regions (e.g., sacrum, centre of the glut, heel, and neck) are at a greater risk of PU formation (Coleman et al., 2014), the accessibility, ease of movement control, and possibility of localized simulation-designed thermal preconditioning make the finger an ideal site to investigate the relationship between temperature and friction and develop a test bench for future applications to PU-relevant skin sites and contact materials. To quantify the temperature distribution of the skin tissue, we used 3D surface scanning and Optical Coherence Tomography (OCT) to develop an anatomically representative thermal model of the finger. Our complementary theoretical and experimental results provide new insight into thermal modulation of skin friction that can be employed in product design and development of thermal technologies to maintain skin integrity.

2. Methods

2.1. Skin friction experiments

We conducted experiments in a climatic chamber with air temperature ~24 °C and relative humidity ~50%. Following on University of Southampton ethical approval (ERGOII 73017), eight healthy participants (4M/4F; age: 29±5y; height: 171 ± 11 cm; body mass: 75 ± 16 Kg) provided informed consent and volunteered to take part in the experiment. Upon arrival to the laboratory, participants underwent an OCT scan (VivoSight Dx OCT System, UK) of their index finger pad to characterise individual variability in the root mean square of the surface roughness (Rq, μm), and epidermal thickness (μm; note: due to technical reasons this was only available in N = 5) (Table 1). Finger pad static contact area (cm^2) was also determined by acquiring ink-based contact images of the finger pad statically-pressed against the experimental plate (normal force: 5N; see further below for details on experimental procedures) and measuring its surface via image processing software (ImageJ, NIH, USA). (Table 1).

Table 1
Individual variability in surface roughness (Rq), finger pad contact area (cm^2), and epidermal thickness (μm; note: due to technical reasons this was only available in N = 5). N.a. = not available.

Participant	*Surface roughness (Rq, μm)*	*Static contact area at 5N (cm^2)*	*Epidermal thickness (μm)*
ID1	1.30	1.32	222.13
ID2	1.44	1.03	276.53
ID3	1.25	0.86	n.a.
ID4	0.76	2.83	208.53
ID5	3.04	1.26	n.a.
ID6	1.43	1.12	n.a.
ID8	1.16	2.76	380.80
ID9	2.70	1.61	253.87
Mean	1.63	1.60	268.37
SD	0.80	0.77	68.26

All participants were then extensively familiarised and trained with the experimental procedures. Participants were required to slide their index finger pad against the surface of a thermally controllable, aluminium friction rig (see **section 2.2**), which was set at either thermo-neutral (24 °C), cold (16 °C), or warm (38 °C) state (note: thermal quality is categorised in relation to air temperature). The sliding movement consisted of actively pulling the finger pad from a fixed starting point (i.e. at the top of the plate) to an end point located 100 mm away on a straight line (i.e. at the bottom of the plate) at a speed of ~3.3 cm s^{-1} (note: this was controlled with a timer). Each participant was required to maintain a stable 5N normal force during the pulling action, using visual feedback from a digital meter described (see **section 2.2**). The rationale for using 5N (e.g. vs. 0.2N employed in prior research on modulation of CoF through heating for haptic applications)(Choi et al., 2022) was that pilot data indicated that participants could more consistently maintain this normal force than lower values, making the small changes in normal load less likely to lead to large change in CoF, as also reported by van Kuilenburg et al. (van Kuilenburg et al., 2015). The consistency in the application of 5N normal force was confirmed by the experimental results (see Fig. 1).

Each participant was instructed to first wash and dry their hands. Then a skin conductance (in μS) test was performed using a capacitance meter on the index finger pad to provide an index of baseline local skin hydration. Second, they were instructed to place their finger at the starting point on the plate and press it down to reach a normal force of 5N. This position was maintained for 60s to allow for adaptation and stabilization of skin temperature in relation to the thermal status of the plate (i.e. set at either 24, 16, or 38 °C) (see **section 2.3** for further justification on thermal preconditioning). Following this adaptation period, the participant was instructed to pull the finger longitudinally across the plate (as detailed above). The finger was then removed from the plate and placed on the conductance meter to determine post-sliding skin hydration levels. Upon completion of the measurement, the finger was thoroughly dried, and a 1min interval was allowed, before the same sliding sequence was repeated. The participant performed this sliding sequence 10 times at each plate temperature (i.e., 24, 16, or 38 °C), resulting in a dataset of 30 sliding movements for each of the 9 participants (i.e. 270 datasets in total).

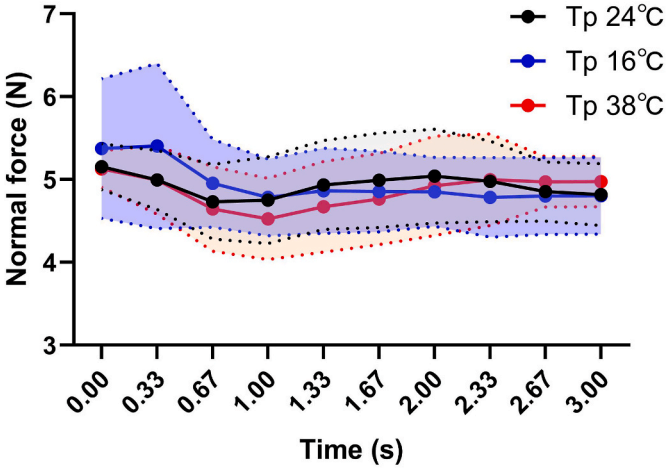

Fig. 1. Group mean (N = 8) ± SD for normal force recorded during the 10 sliding movements for each of the 8 participants at each plate temperature (i.e. 24, 16, and 38 °C). Plate temperature did not have a statistically significant effect on normal force during sliding [2-way ANOVA, main effect of Time: $F_{(2, 14)} = 0.125$; $p = 0.883$].

2.2. Friction rig

Fig. 2 shows the friction rig, which consists of a force plate and low resistance trackway, incorporating calibrated load cells to record both normal and tangential forces, respectively (FS 2050 1500G Load Cell, TE Connectivity, Schaffhausen, Switzerland; LH Series Linear Guides, NSK, Newark, UK; M5 Digital Scale, Dymo, Stamford, CT, US). Force feedback (N) is continually displayed to the participant during interactions using a digital meter interfaced with the load cells (Daisylab, MC computing, USA). A thermally controllable aluminium plate (surface roughness Ra: ~0.3 μm) is mounted upon the force plate and incorporates two Peltier elements (ETH-127-10-13 Peltier Module, Adaptive, Kibworth, UK) that allow PID control of surface temperature via closed-loop, custom-written software (Daisylab, MC computing, USA). The centre of the plate holds a 1-mm hole, allowing for the insertion of an optical probe (Moor Instruments, UK) which is situated at the plate interface. The probe is used for the evaluation of skin blood flow via Laser Doppler Flowmetry (LDF), estimated through a flux value (AUs), whilst the finger is statically compressed against the plate.

Prior to friction measurements, we thermally pre-conditioned the finger for 60s by pressing it at 5N against the plate with pre-set temperature. Laser-Doppler measurements of skin blood flow confirmed that the cutaneous blood cell velocity within the pressed finger was substantially reduced to a plate-temperature independent level (see Fig. S5) (Jay and White, 2005).

The friction rig is interfaced with an A-to-D data acquisition unit (MC computing, USA), sampling plate surface temperature (°C), as well as normal and tangential forces (N), at 33Hz. Accordingly, we used force data to estimate the kinetic coefficient of friction (CoF). The kinetic CoF can be defined as the resistance between two surfaces moving against each other and was calculated for each sliding movement as the ratio of tangential (F_t) to normal force (F_n) according to Amonton's Law (Amontons, 1706):

$$CoF = \frac{F_t}{F_n} \quad \text{(Eq.1)}$$

2.3. The thermal simulations

Section S1 of the Electronic Supplementary Material (ESM) covers geometrical model generation, simulation formulation, and benchmarking in detail. In order to model the temperature distribution within skin tissues, and ensure that thermal-conditioning of the finger prior to sliding would induce meaningful changes in tissue temperature, we developed an anatomical model of the distal and middle phalanges of the index finger of a representative participant (i.e. ID1) pressing on a flat surface that combined realistic 3D detail obtained using two imaging techniques (Shimawaki and Sakai, 2007; He et al., 2008; D'Angelo et al., 2016; Gerling et al., 2013; Zhang et al., 2021) and geometrically simplified features (Lotens, 1992; Shitzer et al., 1996; Walgama, 2005; Fallahi et al., 2017a, 2017b; Wu et al., 2004). We simulated free convection in air and conduction within the finger using the finite element method implemented in Comsol Multiphysics 6.0 (Rykaczewski and Dhanote, 2022) for the three plate temperatures (T_p). We solved the transient convection first and used the resulting flow and temperature fields as inputs for coupled steady-state convection and transient bioheat transfer simulation. We did not explicitly simulate conduction in the substrate because aluminium experiences a negligible change in surface temperature when in contact with a finger (Rykaczewski and Dhanote, 2022). Instead, we accounted for the substrate with a convection boundary condition at the epidermis-metal interface with the equivalent heat transfer coefficient equal to the inverse of the real-to-projected area adjusted 0.0013 $m^2{}^\circ CW^{-1}$ contact resistance (Rykaczewski, 2019). The rest of the simulation setup was based on our prior work (Rykaczewski and Dhanote, 2022) and includes skin-to-environment (at 24 °C) radiation, isothermal tissue initial condition (at 32 °C), and constant boundary condition at the middle and proximal phalanges interface (at 32 °C). We benchmarked the simulations against classical semi-infinite analytical model and in more qualitative terms compared against infrared imaging.

2.4. CoF data analysis

To establish temperature-modulation of CoF amongst participants, we analysed group-level CoF data for the independent and interactive effects of plate temperature (3 levels: 24, 16, or 38 °C) and time (10 levels: 0–0.33s) by means of a 2-way repeated measure ANOVA. Each participant' 10 repeats were averaged for each plate temperature, to allow a group-level analysis based on a N = 9. Furthermore, in order to evaluate the individual variability of temperature-modulation of CoF, we analysed individual CoF data for the independent and interactive effects of plate temperature (3 levels: 24, 16, or 38 °C) and time (10 levels: 0–0.33s) by means of a 2-way repeated measure ANOVA. Post-hoc analyses were performed by means of Tukey's multiple comparisons test.

To establish temperature-modulation of skin conductance (as an index of local skin hydration) as a result of sliding across the plate at varying temperatures, we analysed group-level skin conductance data for the independent and interactive effects of plate temperature (3 levels: 24, 16, or 38 °C) and time (2 levels: pre vs. post sliding) by means of a 2-way repeated measure ANOVA. Each participant' 10 repeats were averaged for each plate temperature, to allow a group-level analysis based on a N = 9. Furthermore, to evaluate the individual variability of

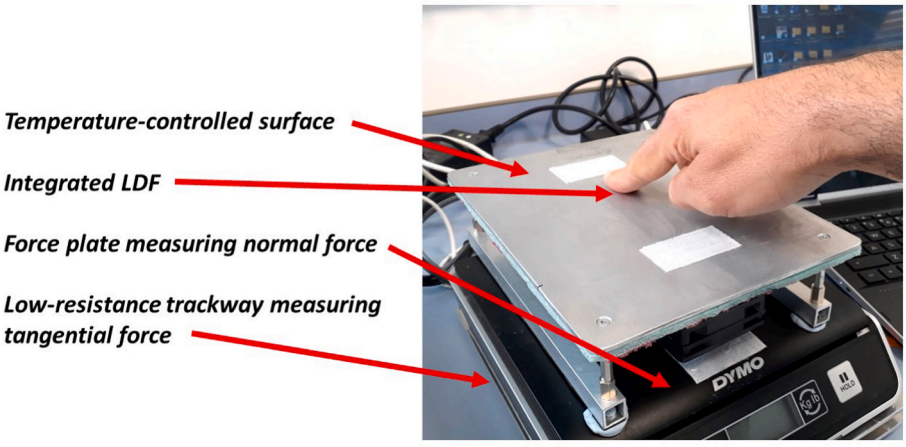

Fig. 2. Friction rig used in the experiments.

temperature-modulation of skin conductance, we analysed individual skin conductance data for the independent and interactive effects of plate temperature (3 levels: 24, 16, or 38 °C) and time (2 levels: pre vs. post sliding) by means of a 2-way repeated measure ANOVA. Post-hoc analyses were performed by means of Tukey's multiple comparisons test.

Finally, to establish potential morphological mechanisms of temperature-modulation of CoF, we assessed the association between the relative change in CoF from 38 vs. 16 °C (i.e. warmest vs. coldest plate temperatures) with finger pad roughness, contact area, and epidermal thickness, by calculating individual Pearson's corelation coefficients.

All data reported in text are mean ± standard deviation (SD) and 95% confidence intervals (95% CIs). Statistical significance was set at $\alpha = 0.05$. All statistical analyses were performed in GraphPad Prism v9.

3. Results

3.1. Theoretical simulations

The thermal simulations allowed us to quantify the spatial and temporal temperature distribution within the finger during the 60s period preceding the sliding movement. The 60-s thermal pre-conditioning step reduces the substantial initial temperature gradients in-plane parallel to the substrate (~5 °C over 0.2 mm) to minor level (under 1 °C over 0.2 mm, see Fig. 3 and equivalent S8 in ESM). Consequently, after the pre-conditioning step, we discuss the 3D internal tissue temperature distribution in terms of temperature averaged in-plane parallel to the plate as a function of vertical distance from the plate.

According to the simulation results, the internal finger temperature was impacted up to around 8 mm by the 60s contact with the plate. The plot in Fig. 4 (and equivalent in S9 in ESM) shows that the epidermis (height of 0–0.43 mm) is within 1 to 1.5 °C of the plate temperature for all the plate settings. From the inner edge of the epidermis layer, the dermis temperature only changed by 1 to 1.5 °C when plate temperature was moderately different from the initial skin temperature (i.e., T_p of 24 °C and 38 °C vs. initial skin temperature of ~32 °C). Thus, for T_p of 24 °C and 38 °C, all of skin tissue (height up to ~1.5 mm) is within 2 to 3 °C of the plate temperature. At the coldest plate setting of 16 °C, the temperature change within the dermis is 3.7 °C, so the corresponding skin tissue was within 5 °C of the plate temperature. From the inner edge of the dermis (~1.5 mm), the temperature of the tissue and bone gradually changed until reaching the initial temperature of 32 °C at a depth of ~8 mm.

3.2. Temperature-modulation of skin CoF

Our experimental friction measurements indicated that, at a group-level (N = 8), the thermally preconditioned sliding finger experienced statistically significantly different CoF(s) as a function of plate temperature and time (temperature x time effect: $F_{(18, 126)} = 2.549$; $p = 0.0013$; Fig. 5a). Specifically, CoF(s) during the sliding movement (i.e. time 0.33–3s) were 0.63 (±0.22 SD), 0.55 (±0.23 SD), 0.43 (±0.21 SD) for the 38 °C, 24 °C, and 16 °C plate temperatures, respectively. By design, normal force during sliding was kept constant at ~5N, and this was confirmed experimentally (mean normal force at 38 °C: 4.9 ± 0.2N; 24 °C: 4.9 ± 0.1N; 16 °C: 4.9 ± 0.2N; no temperature main effect: $F_{(2, 14)} = 0.1254$; $p = 0.8831$; see Fig. 1). Hence, frictional forces during sliding movement (i.e., calculated as CoF x normal force) were on average 13% and 32% lower at 24 °C and 16 °C plate temperatures than during the 38°C-plate interaction, respectively. We also found no group-level differences in skin conductance, and therefore hydration levels, between pre- and post-sliding at each plate temperature (mean difference pre-vs. post-sliding: 0.04 μS [95%CI: -0.23, 0.14]; no time × temperature interaction: $F_{(2,14)} = 0.8326$; $p = 0.455$; Fig. 5b). This observation indicated that sweating- and condensation-induced moisture was unlikely to have appeared/impacted the skin-plate interface and related CoF during sliding.

When considering individual variability in temperature-modulation of skin CoF, we found that 6 out of 8 participants (i.e. 75% of the sample) experienced a statistically significantly lower skin CoF during sliding at 24 and 16 °C than during 38-°C plate interactions (i.e. main effect of temperature $p<0.05$; Fig. 6).

When considering individual variability in temperature-modulation of skin conductance, we found that 50% of the sample (N = 4) experienced temperature-dependent changes in skin conductance (i.e. either increases or decreases) post-sliding (Fig. 7).

When considering the relationship between the relative change in CoF from 38 vs. 16 °C (i.e. warmest vs. coldest plate temperatures) with finger pad's morphological parameters, we found no statistically significant association with neither roughness (Pearson r = 0.43 [95%CI -0.39, 0.87], p = 0.288), contact area (Pearson r = -0.17 [95%CI -0.78, 0.60], p = 0.687), or epidermal thickness (Pearson r = 0.75 [95%CI -0.38, 0.98], p = 0.139).

4. Discussion

Our group-level results demonstrate that skin CoF can be modulated by changing the temperature of the interfacing substrate across a broad temperature range, i.e. 38 to 16 °C (see Fig. 4a.). Our findings expand those of Choi et al. (2022) in relation to the effects of pronounced skin cooling (i.e., <23 °C) on friction, as we observed frictional forces at 16 °C plate temperatures that were 32% lower than during the

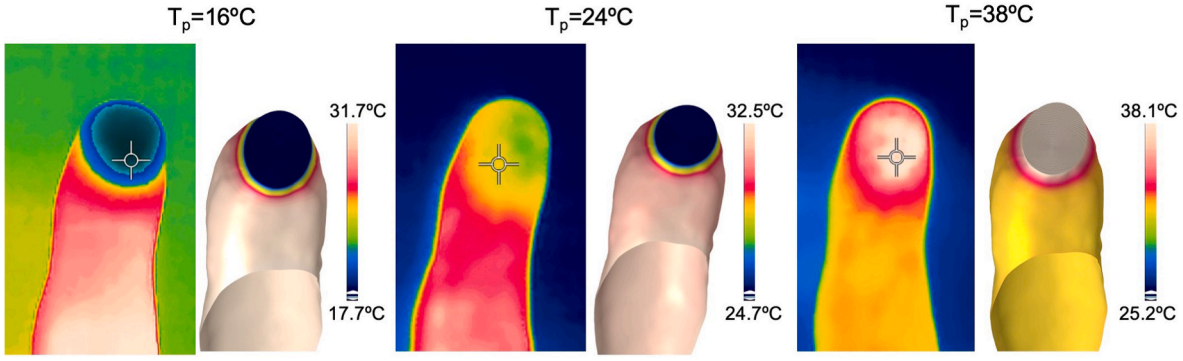

Fig. 3. Comparison between infrared images of the palmar side of the index finger taken shortly after the sliding experiment and of simulated skin surface temperature after 60s of cooling/heating (but in contact with the plate which was hidden in the image). The colormaps and scales in the experimental and simulated temperature maps were synchronized.

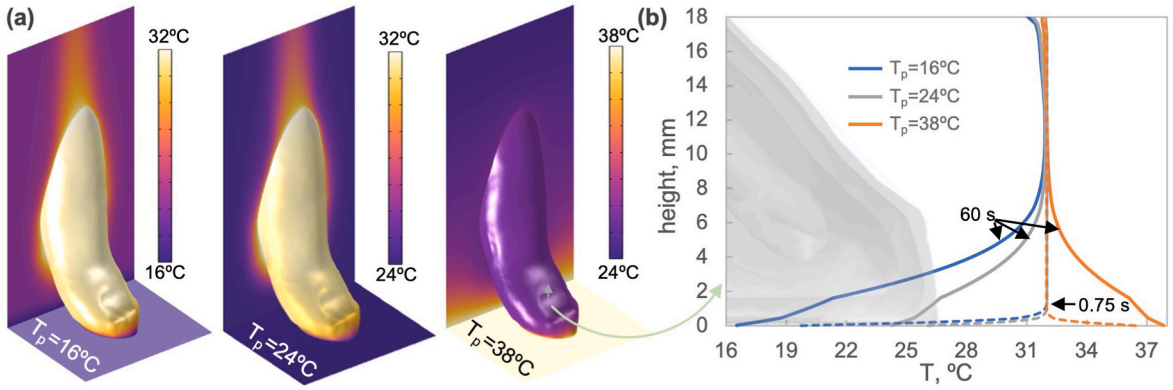

Fig. 4. The modelling results for T_p of 24, 16, and 38 °C: **(a)** surface temperature fields (the temperature scale is adjusted to the full experimental range for each case) and **(b)** temperature of tissue averaged in-plane parallel to the plate as a function of vertical distance from the plate after 0.75s and 60s of pre-conditioning.

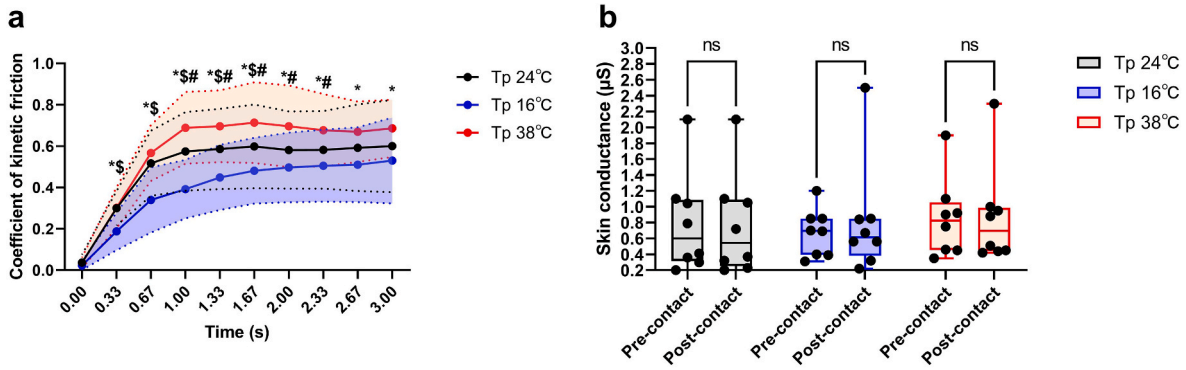

Fig. 5. a. Group mean (N = 8) ± SD (shaded area) for skin CoF recorded during the 10 sliding movements for each of the 8 participants at each plate temperature (i.e. 24, 16, and 38 °C). **b.** Group mean (N = 8) ± SD for skin conductance recorded prior to and immediately after the 10 sliding movements for each of the 8 participants at each plate temperature (i.e. 24, 16, and 38 °C). *p<0.05 for 16 vs. 38 °C; #p<0.05 for 24 vs. 38 °C; $p<0.05 for 16 vs. 24 °C; ns non-statistically significant (p>0.05).

38°C-plate interactions. In contrast to Choi et al. (2022), we observed this group-level phenomenon without large changes in the skin hydration level during sliding (see Fig. 4b). Nevertheless, our main observations presented a degree of individual variability. Specifically, temperature-modulation of skin CoF occurred in 75% of our sample (N = 6/8). Individual variability in temperature-modulation of CoF did not appear to be dependent on variations in finger pad roughness, contact area, or epidermal thickness. Selected increases in moisture at the skin-plate interface may have been a contributing factor for those individual cases where skin CoF did not diminish with plate cooling (see ID5 in Figs. 5 and 6), although this effect was not consistent (e.g. see ID2 in Figs. 5 and 6). Accordingly, our experiments may indicate a predominantly thermal modulation of skin friction and not a correlated skin-moisture and temperature-induced effect.

Choi et al. have hypothesized that temperature changes the mechanical properties of the tissue (which is generally observed (Xu et al., 2008; Bianchi et al., 2022)) relevant to sliding (Choi et al., 2021). Specifically, they observed that T_p increase from 23 °C to 42 °C did not change the interfacial shear strength and explained the ~50% increase in the CoF by increased contact area of the mechanically-softened tissue (Choi et al., 2021). Empirical fitting of their friction data to the Kelvin-Voigt viscoelastic model showed that the temperature increase related to ~143 to 56 MPa viscosity, 15.5 to 10.1 MPa modulus 1, and 5.6 to 5.2 MPa modulus 2 decrease. However, even without changing of the plate temperature from that of the surrounding, sliding changes the contact area of a finger in a complex manner on multiple scales.

Delhaye et al. (2014) showed that after ~100ms of sliding, the apparent finger contact area drops by 30–40% (with normal force of 0.5–2N) and shifts its centroid away from the sliding direction. Potentially due to the increased pressure within the reduced apparent area (normal force remaining constant), Liu et al. (2017) observed using *in-situ* OCT imaging that sliding of a finger (at 6N or ~20–30 kPa) increased the microscale substrate contact along a linear scan from 50% to 88% (i.e., sliding shrank the microscale air gaps). We suspect that the highly heterogeneous mechanical properties of the epidermis, dermis, and adipose tissue can impact these processes in a complex yet not understood manner. The present study revealed that heat transfer to the deeper tissues is non-linear and temperature dependent. Thus, any thermal-induced changes to mechanical properties of skin and fat tissues, and the corresponding contact area, will be complex in nature and requires further multiscale investigation.

The observed thermal modulation of skin friction supports the potential therapeutic benefits of skin cooling regarding minimising friction over vulnerable skin sites. Microclimate conditions at the interface between a loaded skin site at risk of pressure and shear damage (e.g., the sacrum) and a support surface (e.g., a hospital mattress) are commonly associated with ~38 °C skin temperatures (Yilmaz and Günes, 2019), which is equivalent to the warm-plate condition of the current study. Under this real-life scenario, both our 24°C- and 16°C-plate conditions would represent skin cooling stimuli for a warm, mechanically loaded skin site and they could provide meaningful decreases in friction in a dose-dependent fashion (i.e., -13% at 24 °C and -32% at 16 °C), resulting from short periods of pre-conditioning (i.e., 60s). This knowledge could translate to inform the design of user-centred medical devices and wearables, including support surfaces and garments delivering cooling to the skin at a level that is both beneficial and comfortable (Worsley and

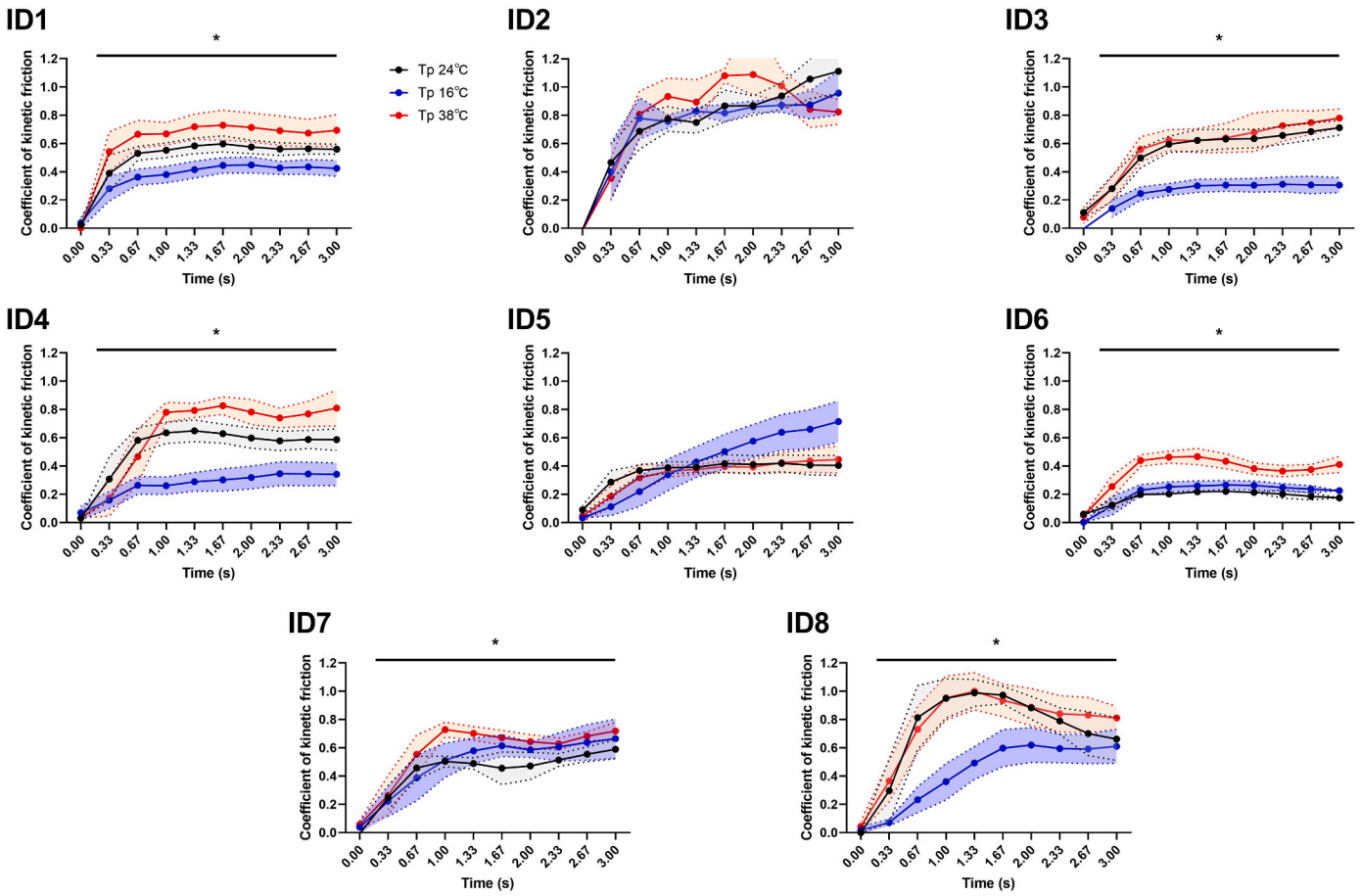

Fig. 6. Individual skin CoF recorded during the 10 sliding movements for each of the 8 participants (ID1-8) at each plate temperature (i.e. 24, 16, and 38 °C). * Statistically significant main effect of temperature on CoF ($p<0.05$).

Bader, 2019b). Indeed, our observed dose-response relationship between skin cooling and friction indicates that friction gains can be obtained at less pronounced levels of cooling (i.e., 24 °C instead of 16 °C), which are less likely to be associated with cold discomfort (Cotter and Taylor, 2005; Filingeri et al., 2014).

Whilst promising, we recognise that our findings apply to the finger and should therefore be interpreted within this small anatomical region. Indeed, the protective effects of cooling to shear-induced damage, as well as its perceptual effects on discomfort, may vary across the human body, due to regional differences in skin biophysics and morphology (Holbrook and Odland, 1974), and in thermoregulatory (Johnson et al., 2014) and perceptual sensitivities (Luo et al., 2020; Holowatz et al., 2010; Guergova and Dufour, 2011). Thus, there may be variations in the efficacy of therapeutic cooling associated with the anatomical site. Furthermore, our experimental setup involved skin interactions with an aluminium plate only. We recognise that the evaluation of temperature modulation of friction using materials more likely used for patient care in chairs and beds (e.g. textiles) is required to translate our findings to clinically meaningful applications. These studies are ongoing in our laboratory. Identifying how the effects of skin cooling vary both physiologically and perceptually over skin sites at greater risk of skin damage and pressure ulcers than the finger, as well as using materials relevant for patient care, will therefore be critical to developing "user-centred" thermal-therapy approaches to maintain skin integrity under mechanical stress that are both effective and comfortable.

5. Conclusions

Our complementary experimental and theoretical results provide new insight into thermal modulation of skin friction and support the potential therapeutic benefits of skin cooling regarding minimising friction over vulnerable skin sites. The methodological approach presented here provides the experimental and theoretical framework upon which to establish differences in the temperature-dependence of skin friction across skin sites more commonly affected by mechanical loading and shear, and with materials used in patient care. This work will inform the development of thermal technologies and products that help maintaining skin integrity under mechanical loading and shearing.

Ethics

The experimental part of this research received ethical approval by UoS as part of application ERGOII 73017.

Data accessibility

Available upon request.

Funding

This work was supported by the Medical Research Council [grant number MR/X019144/1]. AV was supported by a PhD studentship funded by the University of Palermo.

CRediT authorship contribution statement

Alessandro Valenza: Project administration, Methodology, Investigation, Formal analysis, Data curation. **Konrad Rykaczewski:** Writing

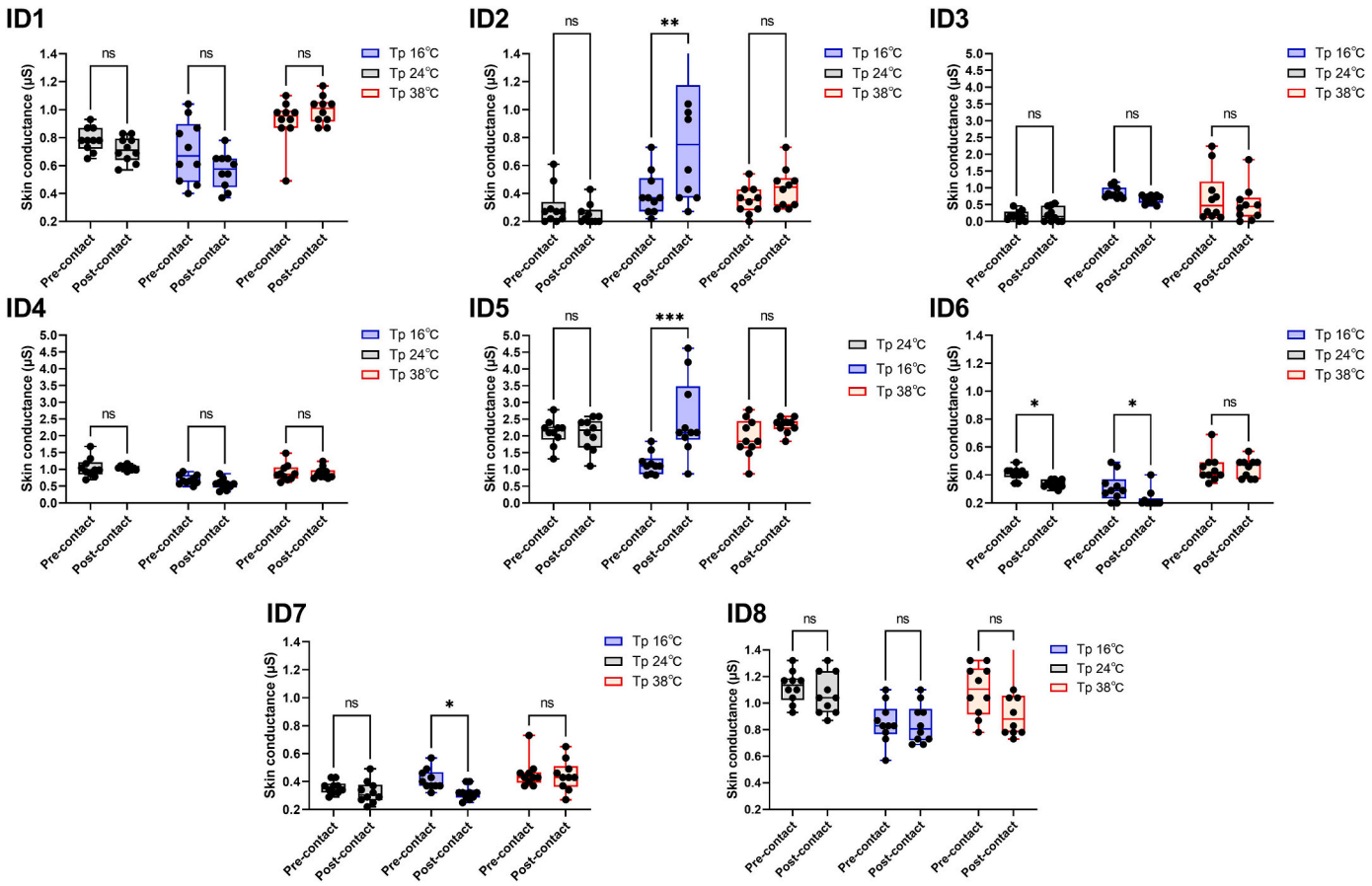

Fig. 7. Individual skin conductance recorded prior to and following the 10 sliding movements for each of the 8 participants (ID1-8) at each plate temperature (i.e. 24, 16, and 38 °C). *p<0.05; **p<0.01; ***p<0.001; ns non-statistically significant (p>0.05).

– original draft, Visualization, Validation, Software, Methodology, Formal analysis, Conceptualization. **Daniel M. Martinez:** Visualization, Software, Methodology. **Antonino Bianco:** Writing – review & editing, Supervision, Resources, Project administration, Conceptualization. **Silvia Caggiari:** Validation, Software, Resources, Methodology, Formal analysis. **Peter Worsley:** Writing – review & editing, Supervision, Resources, Project administration, Data curation, Conceptualization. **Davide Filingeri:** Writing – review & editing, Writing – original draft, Visualization, Supervision, Software, Resources, Project administration, Methodology, Investigation, Formal analysis, Data curation, Conceptualization.

Declaration of competing interest

We declare we have no competing interests.

Data availability

Data will be made available on request.

Acknowledgements:

KR acknowledges Research Computing at ASU for providing High Performance Computing resources that have contributed to the research results reported within this paper. DF wishes to thank Terence Harvey at the national Centre for Advanced Tribology at Southampton for performing measurements of the surface roughness of the friction rig.

Appendix A. Supplementary data

Supplementary data to this article can be found online at https://doi.org/10.1016/j.jmbbm.2023.106072.

References

Amontons G. De la resistance causée dans les machines. Mémoires de l'Académie Royale 257–282, 1706.

André, T., Lefèvre, P., Thonnard, J.-L., 2010. Fingertip moisture is optimally modulated during object manipulation. J. Neurophysiol. 103, 402–408.

Bianchi, L., Cavarzan, F., Ciampitti, L., Cremonesi, M., Grilli, F., Saccomandi, P., 2022. Thermophysical and mechanical properties of biological tissues as a function of temperature: a systematic literature review. Int. J. Hyperther. 39, 297–340.

Choi, C., Ma, Y., Li, X., Ma, X., Hipwell, M.C., 2021. Finger pad topography beyond fingerprints: understanding the heterogeneity effect of finger topography for human–machine interface modeling. ACS Appl. Mater. Interfaces 13, 3303–3310.

Choi, C., Ma, Y., Li, X., Chatterjee, S., Sequeira, S., Friesen, R.F., Felts, J.R., Cynthia Hipwell, M., 2022. Surface haptic rendering of virtual shapes through change in surface temperature. Sci. Robot. 7 https://doi.org/10.1126/SCIROBOTICS.ABL4543/ASSET/5EFD08BB-0817-4436-9F28-ECEC31D8B372/ASSETS/IMAGES/LARGE/SCIROBOTICS.ABL4543-F4.JPG).

Clark, M., 2018. Microclimate: rediscovering an old concept in the aetiology of pressure ulcers. In: Romanelli, M., Clark, M., Gefen, A., Ciprandi, G. (Eds.), Science and Practice of Pressure Ulcer Management, 110. Springer London, London, p. 103. https://doi.org/10.1007/978-1-4471-7413-4_8.

Coleman, S., et al., 2014. A new pressure ulcer conceptual framework. J. Adv. Nurs. 70, 2222–2234. https://doi.org/10.1111/jan.12405.

Cotter, J., Taylor, N., 2005. The distribution of cutaneous sudomotor and alliesthesial thermosensitivity in mildly heat-stressed humans: an open-loop approach. J. Physiol. 565, 335–345. https://doi.org/10.1113/jphysiol.2004.081562.

Delhaye, B., Lefevre, P., Thonnard, J.-L., 2014. Dynamics of fingertip contact during the onset of tangential slip. J. R. Soc. Interface 11, 20140698.

D'Angelo, M.L., Cannella, F., Bianchi, M., D'Imperio, M., Battaglia, E., Poggiani, M., Rossi, G., Bicchi, A., Caldwell, D.G., 2016. An integrated approach to characterize the behavior of a human fingertip in contact with a silica window. IEEE Trans Haptics 10, 123–129.

Fallahi, A., Salimpour, M.R., Shirani, E., 2017a. A 3D thermal model to analyze the temperature changes of digits during cold stress and predict the danger of frostbite in human fingers. J. Therm. Biol. 65, 153–160.
Fallahi, A., Salimpour, M.R., Shirani, E., 2017b. Analytical expressions for estimating endurance time and glove thermal resistance related to human finger in cold conditions. J. Therm. Biol. 69, 334–340.
Filingeri, D., Redortier, B., Hodder, S., Havenith, G., 2014. Thermal and tactile interactions in the perception of local skin wetness at rest and during exercise in thermo-neutral and warm environments. Neuroscience 258, 121–130. https://doi.org/10.1016/j.neuroscience.2013.11.019.
Gerhardt, L., Mattle, N., Schrade, G.U., Spencer, N.D., Derler, S., 2008. Study of skin–fabric interactions of relevance to decubitus: friction and contact-pressure measurements. Skin Res. Technol. 14, 77–88.
Gerling, G.J., Rivest II, Lesniak, D.R., Scanlon, J.R., Wan, L., 2013. Validating a population model of tactile mechanotransduction of slowly adapting type I afferents at levels of skin mechanics, single-unit response and psychophysics. IEEE Trans Haptics 7, 216–228.
Guergova, S., Dufour, A., 2011. Thermal sensitivity in the elderly: a review. Ageing Res. Rev. 10, 80–92.
Guest, J.F., Fuller, G.W., Vowden, P., 2020. Cohort study evaluating the burden of wounds to the UK's National Health Service in 2017/2018: update from 2012/2013. BMJ Open 10, 45253. https://doi.org/10.1136/bmjopen-2020-045253.
He, Y., Liu, H., Himeno, R., Sunaga, J., Kakusho, N., Yokota, H., 2008. Finite element analysis of blood flow and heat transfer in an image-based human finger. Comput. Biol. Med. 38, 555–562.
Holbrook, K.A., Odland, G.F., 1974. Regional differences in the thickness (cell layers) of the human stratum corneum: an ultrastructural analysis. J. Invest. Dermatol. 62, 415–422. https://doi.org/10.1111/1523-1747.ep12701670.
Holowatz, L.A., Thompson-Torgerson, C., Kenney, W.L., 2010. Aging and the control of human skin blood flow. Front. Biosci. 15, 718.
Jan, Y.K., 2020. The effects of local cooling rates on perfusion of sacral skin under externally applied pressure in people with spinal cord injury: an exploratory study. Spinal Cord 58, 476–483. https://doi.org/10.1038/s41393-019-0378-x.
Jay, O., White, M.D., 2005. The effect of local finger contact pressure upon cutaneous blood perfusion of the fingertip at different skin temperatures. In: 11th International Conference on Environmental Ergonomics, pp. 364–367.
Johnson, J.M., Minson, C.T., Kellogg, D.L., 2014. Cutaneous vasodilator and vasoconstrictor mechanisms in temperature regulation. Compr. Physiol. 4, 33–89. https://doi.org/10.1002/cphy.c130015.
Kokate, J.Y., Leland, K.J., Held, A.M., Hansen, G.L., Kveen, G.L., Johnson, B.A., Wilke, M. S., Sparrow, E.M., Iaizzo, P.A., 1995. Temperature-modulated pressure ulcers: a porcine model. Arch. Phys. Med. Rehabil. 76, 666–673. https://doi.org/10.1016/S0003-9993(95)80637-7.
Lachenbruch, C., 2005. Skin cooling surfaces: estimating the importance of limiting skin temperature. Ostomy/Wound Manag. 51, 70–79.
Liu, X., Maiti, R., Lu, Z.H., Carré, M.J., Matcher, S.J., Lewis, R., 2017. New non-invasive techniques to quantify skin surface strain and sub-surface layer deformation of finger-pad during sliding. Biotribology 12, 52–58.
Lotens, W.A., 1992. Simulation of hand cooling due to touching cold materials. Eur. J. Appl. Physiol. Occup. Physiol. 65, 59–65.
Luo, M., et al., 2020. High-density thermal sensitivity maps of the human body. Build. Environ. 167 https://doi.org/10.1016/j.buildenv.2019.106435.
Rykaczewski, K., 2019. Modeling thermal contact resistance at the finger-object interface. Temperature 6, 85–95.
Rykaczewski, K., Dhanote, T., 2022. Analysis of thermocouple-based finger contact temperature measurements. J. Therm. Biol., 103293
Shimawaki, S., Sakai, N., 2007. Quasi-static deformation analysis of a human finger using a three-dimensional finite element model constructed from CT images. J. Environ. Eng. 2, 56–63.
Shitzer, A., Stroschein, L.A., Gonzalez, R.R., Pandolf, K.B., 1996. Lumped-parameter tissue temperature-blood perfusion model of a cold-stressed fingertip. J. Appl. Physiol. 80, 1829–1834.
Tzen, Y.T., Brienza, D.M., Karg, P.E., Loughlin, P.J., 2013. Effectiveness of local cooling for enhancing tissue ischemia tolerance in people with spinal cord injury. J. Spinal Cord Med. 36, 357–364. https://doi.org/10.1179/2045772312Y.0000000085.
van Kuilenburg, J., Masen, M.A., van der Heide, E., 2015. A review of fingerpad contact mechanics and friction and how this affects tactile perception. In: Proceedings of the Institution of Mechanical Engineers, Part J: Journal of Engineering Tribology, vol. 229, pp. 243–258.
Walgama, C., 2005. Simulation of Hand Cooling in Contact with Cold Materials.
Worsley, P.R., Bader, D.L., 2019a. A modified evaluation of spacer fabric and airflow technologies for controlling the microclimate at the loaded support interface. Textil. Res. J. 89, 2154–2162. https://doi.org/10.1177/0040517518786279.
Worsley, P.R., Bader, D.L., 2019b. A modified evaluation of spacer fabric and airflow technologies for controlling the microclimate at the loaded support interface. Textil. Res. J. 89, 2154–2162.
Worsley, P.R., Hanneke, Crielaard, Oomens, C.W.J., Bader, D.L., 2020. An evaluation of dermal microcirculatory occlusion under repeated mechanical loads: implication of lymphatic impairment in pressure ulcers. Microcirculation 27, e12645. https://doi.org/10.1111/micc.12645.
Wu, J.Z., Dong, R.G., Rakheja, S., Schopper, A.W., Smutz, W.P., 2004. A structural fingertip model for simulating of the biomechanics of tactile sensation. Med. Eng. Phys. 26, 165–175.
Xu, F., Seffen, K.A., Lu, T.J., 2008. Temperature-dependent mechanical behaviors of skin tissue. IAENG Int. J. Comput. Sci. 35.
Yilmaz, İ., Günes, Ü.Y., 2019. Sacral skin temperature and pressure ulcer development: a descriptive study. Wound Manag Prev 65, 30–37.
Zhang, M., Li, R., Li, J., Wang, F., Subramaniam, S., Lang, J., Passalacqua, A., Song, G., 2021. A 3D multi-segment thermoregulation model of the hand with realistic anatomy: development, validation, and parametric analysis. Build. Environ. 201, 107964.